Original Research Article

Corrosion behavior of welded joints of X70 pipeline steel produced by high-frequency welding

Abstract: Corrosion behavior of welded joints of steel pipe category X70 produced by high-frequency welding, in different conditions, in which it is possible to initiate stress-corrosion cracking, hydrogen or sulfide cracking, was investigated. According to the results of electrochemical researches, the kinetic parameters of the cathode and anode processes on the surface of the welded joint of pipe in the investigated solutions are determined. Corrosion resistance of the welded joint HFW-pipe is similar to corrosion resistance of the base metal.

Key words: *pipe, high-frequency welding, corrosion, stress-corrosion cracking, corrosion potential*

Introduction.

It is well-known that pipes of big diameter from 530 to 1420 mm for pipelines are manufactured using arc welding under flux [1-3]. In this case the effectively of such type of welding significantly decreasing with decreasing of the thick of pipe wall. Moreover, taking into the account the obligatory implementation of double-sided welding, the equipment for arc welding is considerably complicated, due to the need to transport flux inside the pipe. This contributed to the intensive development of high-frequency welding (HFW) method, primarily for small and medium diameter pipes. Up to date, in the world, with the HFW technology produces pipes of the categories from X65 to X80 with the diameter from 219 to 660 mm and wall thickness up to 25,4 mm. Despite the rapid development of this technology, at the present time in the scientific and technical literature there is virtually no information on the corrosion resistance of the welded joints of HFW-pipes.

The purpose of this work was to investigate the corrosion behavior of welded joints of HFW-pipe, on the example of Ø508.0 × 8.7 mm pipe from a steel of category X70, in the conditions where initiation of stress-corrosion cracking, hydrogen or sulfide cracking is possible. The method of voltammetric measurements evaluated the electrochemical properties of the weld zone and the base metal of the HFW-pipe in media with different aggressiveness, and also tested for resistance to hydrogen sulfide cracking.

Materials and methods.

The chemical composition of the investigated material was determined by the spectral method on the device "Spectrovak-1000" produced by the company "Baird". The chemical composition of rolling steel is shown in Table 1.

Table 1 - Chemical composition of the base metal of HFW-pipe

Chemical composition, wt-% max											
C	***Si***	***Mn***	***P***	***S***	***V***	***Nb***	***Ti***	***Ni***	***Cr***	***Al***	***Cu***
0,08	0,22	1,34	0,014	0,006	0,040	0,06	0,014	0,19	0,22	0,037	0,02

Metallographic research of the microstructure were carried out on the microscope "Neofot-21" after the microsection etching in the nital.

Electrochemical measurements.

The evaluation of the corrosion resistance of the welded joint of the HFW-pipe in various media were carried out by the method of polarization curves. As a rule, from the experience of operating oil and gas pipelines, stress-corrosion cracking occurs in the environment with a hydrogen index close to neutral [4-6]. Thereby, the tests were carried out in three solutions with a hydrogen index in the range from 5.4 up to 8.4: 3% NaCl, pH 6,8 [4] (solution №1); 0,037 g/l KCl+0,559 g/l $NaHCO_3$+0,008 g/l $CaCl_2$+0,089 g/l $MgSO_4 \cdot 7H_2O$, pH 8,2-8,4 [5-6] (solution №2); 1,92 g/l HCOOH + 54,5 g/l HCOONa + 10 g/l KCNS, pH 5,4 [7] (solution №3).

Electrochemical researches were carried out on the microsection of the welded joints of the HFW-pipe Ø508,0 × 8,7 mm in the size of 50×20×8,7 mm, with the fusion zone in the middle. Before research, samples were sanded with sandpaper of different grain sizes from 320 to 1000, then washed with running and distilled water and rubbed with alcohol. On the surface of the welded joint area of 5 mm^2 installed clamping electrochemical cell, the other surface was protected by an insulating coating. Measurement was carried out according to the three electrode scheme: working electrode (WE) - basic metal and weld joint; auxiliary electrode (AE) - platinum, comparison electrode (CE) - chlorine-silver electrode. The polarization curves were measured in dynamical mode at the speed of potential sweep of 0.0005 V/s. The polarization range from the corrosion potential was 1.5 V to the cathode side and 2.0 V to the anode. The time for measuring the potential of the corrosion potential of the working sample was 60 minutes, after which the potential for scanning was switched on. From the received polarization curves were determined corrosion potential, the current in the region of active anode dissolution for the potential -0.5 V ($i_{-0.5\,V}$), the Tafel slope of the initial part of the anode curve (b_a), the limiting diffusion current (i_d) and the

potential for initiating the release of hydrogen (E_{H_2}). In analyzing the influence of the protective potential on the corrosion of the surface of the pipe under the protective cover, it is proposed to determine the current density of the cathode protection (j_{cp}) and compare it with the density of the limiting current of oxygen recovery (j_{O_2}) [8]. If the ratio of currents is less than 1, corrosion of the pipe wall in the coating defect is possible; if the ratio of currents is in the range from 1 to 3 - protective effect is achieved. Further increase in the current density of the cathode protection does not lead to a significant reduction in the rate of corrosion, but is accompanied by a sharp increase in the volume of hydrogen which is formed during the decomposition of the electrolyte.

Investigation of the resistance of the welded joint of HFW-pipe against hydrogen cracking and hydrogen sulfide corrosion cracking.

According to the requirements of ANSI / API specification 5L [9], corrosion researches are carried out, by the results of which corrosion rate of the metal in an environment that containing hydrogen sulfide, as well as its resistance to hydrogen cracking (HC) and hydrogen sulfide cracking (HSC) is determined. Tests for resistance to HC were conducted in accordance with NACE TM 0284-2003 [10] for 96 hours. After the tests, each sample was cut into 3 equal parts. Metallographic specimen was made, and the rate of total corrosion, Crack Length Ratio (CLR), Crack Thickness Ratio (CTR), which, accordingly, should not exceed 0.5 mm/year, were determined, CLR-6 % and CTR - 3%.

$$CLR = \frac{\sum a}{W} \cdot 100 \ \% \quad (1)$$

$$CLR = \frac{\sum b}{T} \cdot 100 \ \% \quad (2)$$

where a - length crack, b - thickness crack, W - section width, T - test specimen thickness.

For tests of resistance to hydrogen sulfide cracking (HSC), the samples were made in such a way that one of the surfaces is located at the minimum possible distance from the inner surface of the pipe. Tests were conducted into the accordance to NACE TM 0177-2005 (method B, ISO 7539-2-89) for 720 hours [11]. The load level was equal. The criterion of resistance to HSC is the absence of cracks.

Results and discussion.

The microstructure of the fusion zone of the HFW-pipe Ø508.0 × 8.7 mm from steel of category X70 is shown in Figure 1. The fusion line represents a distinct continuous carbon-free light band. Due to the local thermal treatment of coarse-grained lamellar or needle structure that formed after welding in the

zone of thermal influence, transforms into fine-grained ferrite-perlite. The amount of perlite component in the structure is determined by the carbon content of the steel.

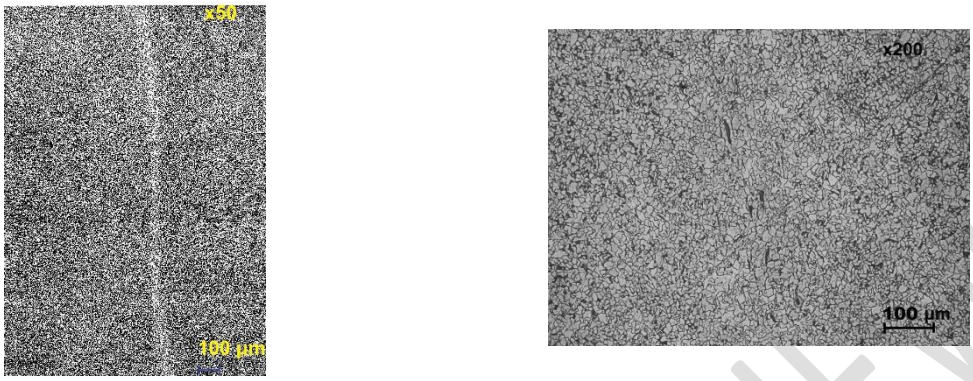

Figure 1 - Microstructure of the fusion zone of the HFW-pipe welded joint Ø508.0 × 8.7 mm from steel category X70 after etching in the nital

The microstructure of the base metal and the heat affected zone of the pipe is a fine-grained ferrite-perlite mixture with enough highlighted strips (Figure 2).

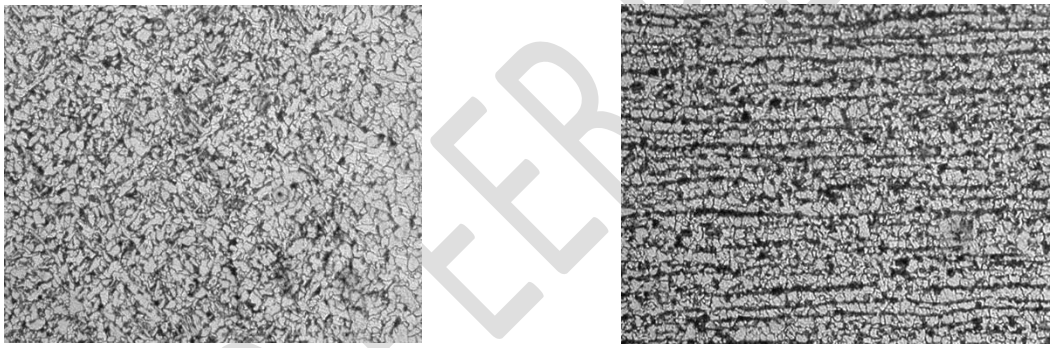

a) *b)*

Figure 2 – Microstructure of the base metal of the HFW-pipe Ø508,0 × 8,7 mm from steel category X70, heat affected zone (a) and base metal (b) after etching in 4% nital, × 200

Figures 3, 4 and 5 shows the dynamics of changes in the corrosion potential (a) and the polarization curves (b) of the base metal (BM) and the welding joint (WJ) of the HFW-pipe in solutions № 1, № 2 and № 3, respectively. As can be seen from the curves presented Fig. 3a, the corrosion potentials on BM and WJ are close in value and are -0.570 V and -0.584 V respectively. The behavior of the anode and cathode curves of the two welded zones is similar Fig. 3b. The numerical values of the electrochemical parameters of the cathode and anode processes, that was determined graphically from Fig. 3b, is shown in Table 2. From the corrosion potential up to 0.5 V for both zones in this solution, is characterized a wide area of active dissolution. There is a slightly smaller angle of the Tafel slope of the starting zone of the anode curve of WJ zone in comparison the BM, which indicates a higher rate of anode

dissolution under the same conditions. For potentials larger than -0.25 V, the deceleration of the anode dissolution was observed due to passivation of the surface of the sample.

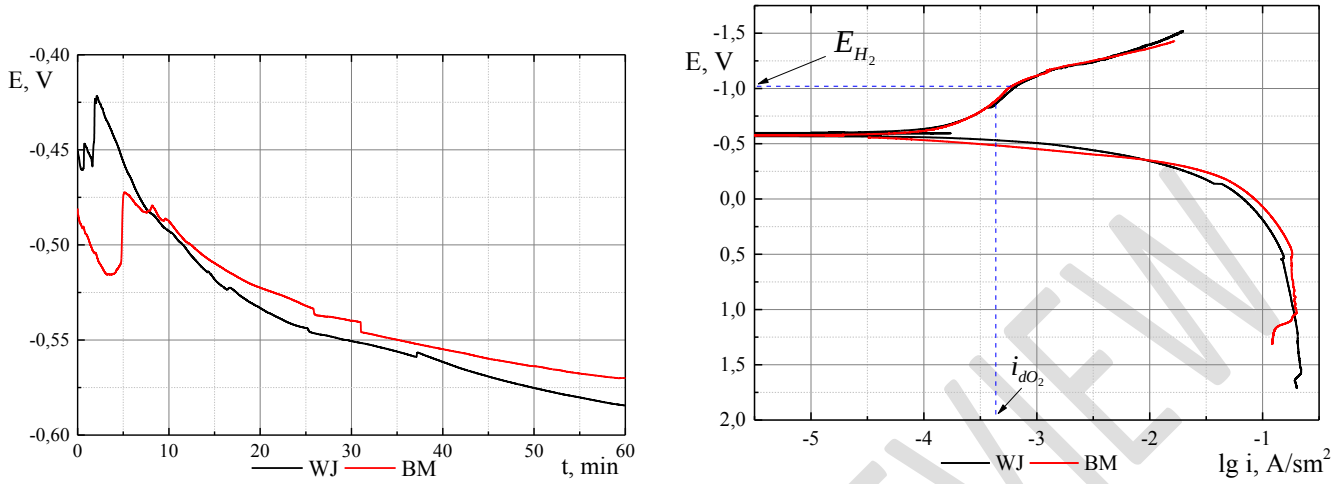

а *б*

Figure 3 **-** Changes in corrosion potential in time (a) and the polarization curves (b) BM and WJ of the sample of the HFW-pipe in solution №1.

In the solution №2, BM is characterized by a sharp shift of the corrosion potential in the region of negative values from -0.455 V that stabilizes after 60 minutes at -0.641 V, and on the WJ were shifted smoothly from -0.490 V, and stabilizes at -0.596 V, Fig. 4a. This difference in potentials is significant, but considering the much smaller area of the WJ as compared to the BM, it does not pose any danger in terms of the development of local corrosion processes. The area of active dissolution is long enough for both zones - from the potential of corrosion to the potential is about -0.25 V, above which there is a slowing down of the anode process due to the surface shielding by products of corrosion. The Tafel's angles of slope of the initial regions of the anode curves indicate a higher rate of dissolution of the BM in comparison with the WJ.

In solution № 3, the dynamics of the change in corrosion potentials within 60 minutes is characterized by a slight displacement in the region of positive values for both the BM and the WJ, varying from -0.632 V up to -0.604 V and -0.636 V up to -0.622 V, respectively. The electrochemical characteristics of the anode and cathode processes on the BM and the WJ are shown in Table 2. The analysis of the course of the anode curves shows that the rate of dissolution of the WJ at the potential -0.5 V is almost 6 times higher than the BM (Table 2**)**. Both zones are characterized by the area of active dissolution: for the BM in the range from -0.543 to -0.03 V; for the WJ – from -0.588 to 0.25 V.

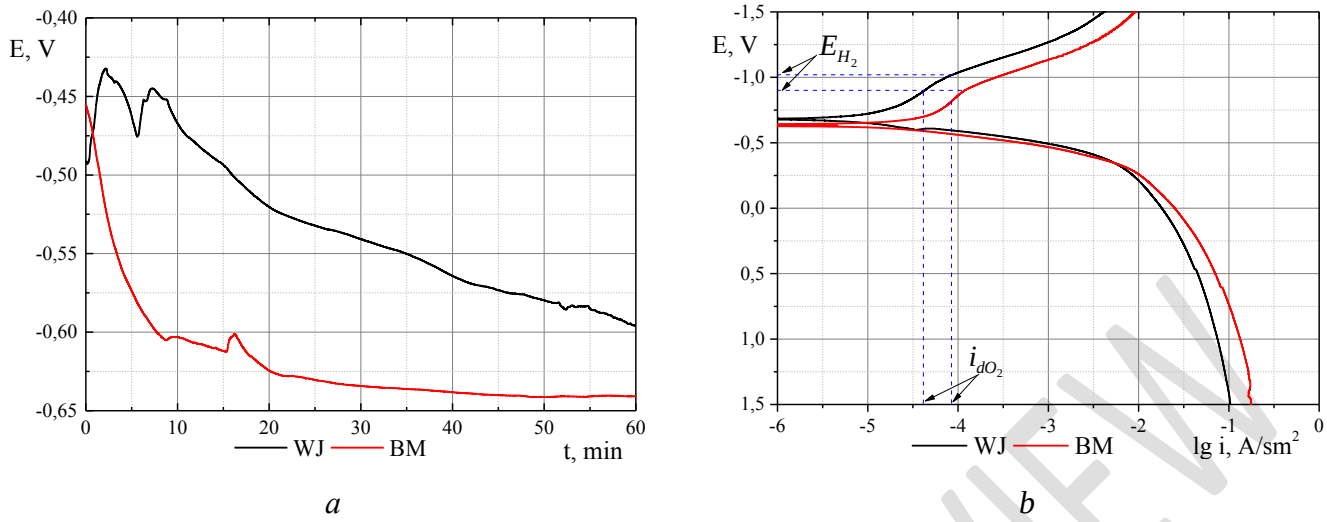

Figure 4 - Changes in corrosion potential in time (a) and the polarization curves (b) of the BM and the WJ of the sample of the HFW-pipe in solution №2

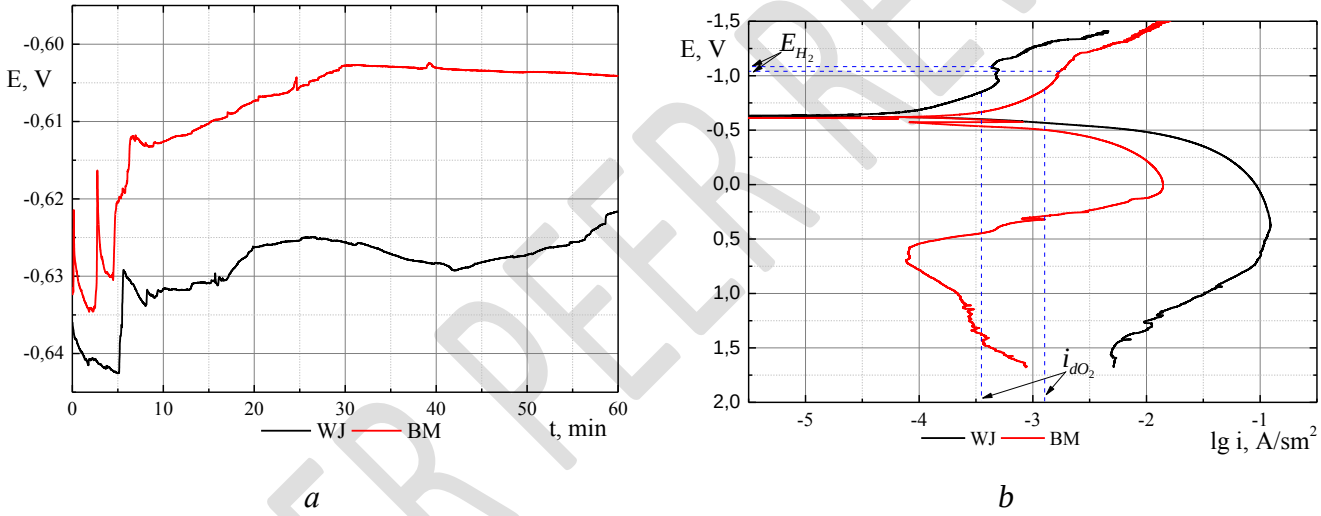

Figure 5 - Changes in corrosion potential in time (a) and polarization curves (b) of the BM and the WJ of the sample of the HFW-pipe in solution №3

The analysis of the ratio of currents j_{cp} / j_{O_2} for the region of the WJ and the BM were conducted in order to determine the possible formation on the surface of the pipe under peeling coating of local areas with different electrochemical activity. The results of the analysis are shown in Table 2.

From the analysis of experimental data it can be concluded that in the range of protective potentials (from -0.85 V up to -1.15 V relative to copper-sulfate electrode comparison, which corresponds the value from -0.75 V to -1.05 V relative to the chlorine-silver electrode comparison), the ratio of currents j_{cp} / j_{O_2} in solutions № 1-3, both on the BM and on metal of the WJ is more than 1 by the polarization potential, which is approaching the maximum protective value. Such conditions contribute to the decomposition of

the electrolyte with hydrogen release. But it should be noted that the ratio of currents j_{cp} / j_{O_2} for the BM and the WJ practically does not differ. This indicates that when working under the conditions of cathodic protection of hydrogen absorption of the weld and base metal is not expected.

The results of the study of the resistance of the welded joint of the HFW-pipe to the HC and the HSC are given in Table 3.

Table 2 - Electrochemical characteristics of different zones of the HFW-pipe in solutions №1-3

Solution	Zone	Electrochemical characteristics				Currents of cathode protection, A/m^2		Ratio j_{cp} / j_{O_2}	
		anode		cathode					
		$i_{-0.5\ B}$, A/м^2	b_a, B	i_d, A/м^2	E_{H_2}, B	for cathode potentials -0,75 V	for cathode potentials -1,05 V	for cathode potentials -0,75 V	for cathode potentials -1,05 V
№1	BM	$1{,}1\times10^{-3}$	0,069	0,0007	-1,03	$2{,}8\times10^{-4}$	$7{,}6\times10^{-4}$	0,4	1,08
	WJ	$3{,}1\times10^{-4}$	0,054	0,0007	-1,03	$2{,}8\times10^{-4}$	$7{,}6\times10^{-4}$	0,4	1,08
№2	BM	$1{,}2\times10^{-4}$	0,074	$8{,}2\times10^{-5}$	-0,94	$4{,}5\times10^{-5}$	$2{,}6\times10^{-4}$	0,5	3,2
	WJ	$8{,}1\times10^{-4}$	0,087	$3{,}8\times10^{-5}$	-1,0	$1{,}5\times10^{-5}$	$1{,}1\times10^{-4}$	0,4	2,9
№3	BM	$1{,}2\times10^{-3}$	0,057	$1{,}5\times10^{-3}$	-1,2	$7{,}1\times10^{-4}$	$1{,}8\times10^{-3}$	0,5	1,2
	WJ	$6{,}8\times10^{-3}$	0,069	$5{,}0\times10^{-4}$	-1,2	$2{,}5\times10^{-4}$	$4{,}9\times10^{-4}$	0,5	1,0

Table 3 - Indicators of corrosion resistance of the BM and the WJ metal of HFW-pipes

Zone	Indicators of corrosion resistance			
	Corrosion rate, mm/year	HC		HSC at $0{,}7\sigma_{0,2}$
		CLR, %	CTR, %	
BM	0,5	3,2-3,7	2,0-2,3	Cracks are not detected
WJ	-	0,0	0,0	Cracks are not detected

The results obtained in Table 3 show that the welded joint of the HFW-pipe is resistant to HC and HSC by the determined parameters (corrosion rate, CLR, CTR, HSC resistance at 0.7σ 0.2 for 720 hours).

Conclusions

1. The mechanism of anodic dissolution of both the base metal and the welding joint is controlled by diffusion of oxygen, which is confirmed by the values of the Constants of Tafel (from 0.054 V to 0.087 V). Differences in the values of the observed Tafel's slopes, indicate a greater or lesser speed of this process. Such anode behavior indicates that the corrosion resistance of the welded joints of the HFW-pipes in general is similar to the corrosion resistance of the base metal.

2. The potential for the initiation of hydrogen release in the range of pH from 5.4 to 8.2 is approximately similar for the base metal and for the weld joint.

3. In the range of protective potentials in solutions of different aggressiveness, the ratio of the current of cathode protection to the boundary diffusion current j_{cp} / j_{O_2} for the base metal and the weld joint does not differ. Thus, in the conditions of cathodic protection, flooding of the base metal and the weld is not expected.

Summing up the above, it can be argued that when operation a pipeline constructed using high-frequency welding technology under pressure in the conditions of cathodic protection, the resistance of welded joints to stress-corrosion cracking will depend only on the protective properties of the insulating coating.

References

1. Zeng Huilin, Wang Changjiang, Yang Xuemei, Wang Xinsheng, Liu Ran. Automatic welding technologies for long-distance pipelines by use of all-position self-shielded flux cored wires//Natural Gas Industry B. – Vol. 1, Issue 1, October 2014, Pages 113-118.

2. Yongchang Liu, Yi Shao, Chenxi Liu, Yan Chen, Dantian Zhang. Microstructure Evolution of HSLA Pipeline Steels after Hot Uniaxial Compression//Materials (Basel). 2016 Sep; 9(9): 721.

3. Satish Kumar Sharma, Sachin Maheshwari. A review on welding of high strength oil and gas pipeline steels//Journal of Natural Gas Science and Engineering. – Vol. 38, February 2017, Pages 203-217February 2017, Pages 203-217.

4. Technical challenges of heavy wall HFW-pipe production for Bord gáis éireann pipeline project. /Paul O'Dwyer, Athanasios Tazedakis, Peter Boothby/ Proceedings of the 8th International Pipeline Conference IPC2010. September 27-October 1, 2010, Calgary, Alberta, Canada. IPC 2010-31293

5. Szklarska-Smialowska K Z., Xia Z., Rebak R.B. Technical note: stress corrosion cracking of X-52 carbon steel in dilute aqueous solutions/ Corrosion. –Vol.50. – No.5. – 1994. – P.334-338.

6. Jinheng Luo, Sheji Luo, Lifeng Li, Liang Zhang, Gang Wu, Lixia Zhu. Stress corrosion cracking behavior of X90 pipeline steel and its weld joint at different applied potentials in near-neutral

solutions/Natural Gas Industry B.-Available online 16 March 2019, open access. https://www.sciencedirect.com/science/article/pii/S2352854019300270

7. Lubenskij A.P.; Lubenskij S.A.; CHeburahtin N.A.; Antonov V.G. Lubenskij. Sostav dlya provedeniya ispytanij na stojkost' trubnyh stalej k korrozionnomu rastreskivaniyu pod napryazheniem. Patent RF № 2082154. – Zayavl. 12.07.1994. – Opubl. 20.06.1997.

8. Hizhnyakov V.I. Korrozionnoe rastreskivanie napryazhenno-deformirovannyh truboprovodov pri transporte nefti i gaza / V.I. Hizhnyakov, YU. A. Kudashkin, M.V. Hizhnyakov, A.V. ZHilin. // Izvestiya Tomskogo politekhnicheskogo universiteta. Himiya. – 2011. – T. 319. – № 3. – S. 84-89.

9. ANSI/APISpec.5L:2007/ISO 3183:2007. Specification for Line Pipe. Petroleum and natural gas industries—Steel pipe for pipeline transportation systems.

10. NACE TM 0284-2003 Standard Test Method Evaluation of Pipeline and Pressure Vessel Steels for Resistance to Hydrogen-Induced Cracking

11. NACE TM 0177-2005 Standard Test Method Laboratory Testing of Metals for Resistance to Sulfide Stress Cracking and Stress Corrosion Cracking in H2S Environments